

Original Research

Carbonized Waste Corrugated Paper Packaging Boxes as Low-Cost Adsorbent for Removing Aqueous Pb(II), Cd(II), Zn(II), and Methylene Blue

Zhuhong Ding^{1*}, Xuebin Xu¹, Thihongnhung Phan¹, Xin Hu²

¹School of Environmental Science and Engineering, Nanjing Tech University, Nanjing, P.R. China

²State Key Laboratory of Analytical Chemistry for Life Science, Center of Material Analysis and School of Chemistry and Chemical Engineering, Nanjing University, Nanjing, P.R. China

Received: 28 September 2017

Accepted: 14 December 2017

Abstract

A common solid waste – corrugated-paper packaging boxes – was carbonized at 300, 450, and 600°C to develop low-cost adsorbents (biochars). The resulting adsorbents were characterized and their adsorption performances were evaluated by the batch sorption of aqueous Pb(II), Zn(II), Cd(II), and methylene blue (MB). The biochar obtained at 600°C exhibited larger specific surface area, higher mineral contents, and pH of zero point charge (pHPZC). Calcium carbonate, lead carbonate/basic, and zinc carbonate were observed in the metal-sorbed biochars by a power X-ray diffractometer (XRD). The biochar of higher pyrolysis temperature (600°C) had high sorption capacity of aqueous Pb(II), Zn(II), and Cd(II) with the Langmuir maximum sorption capacity of 458, 146, and 10.7 mg g⁻¹, respectively. The pseudo-second-order model gave a better fit for the kinetic data of Pb(II), Zn(II), Cd(II), and MB onto the biochar (600°C). Moreover, the electrostatic attraction was the dominant mechanism for adsorption of MB while precipitation could be the main mechanisms for adsorption of Pb(II), Zn(II), and Cd(II). Therefore, carbonization can be an efficient and value-addition method for the recycling of waste corrugated paper packaging boxes and for the low-cost wastewater treatment.

Keywords: waste packaging box, recycling, heavy metals, dye, sorption

Introduction

Due to increasing public awareness on environmental issues, the recycling of solid waste, a kind of discarded resource, has received more and more attention recently.

It has been reported that 66.8 percent of paper consumed in the United States was recovered for recycling in 2015 (paperrecycles.org). Generally, waste paper contains not only cellulose but also fillers (e.g., calcium carbonate or aluminosilicates) and organic/inorganic adhesives (e.g., corn starch or polyvinyl alcohol) to improve their properties [1]. The traditional recycling of waste paper is made into paper-based packaging and other recycled papers (paperrecycles.org). In recent years,

*e-mail: dzuhong@njtech.edu.cn

new value-added utilization of the waste paper has also been investigated as adsorbents [2], energy storage material [3], textiles [4], renewable fuel [5], and so on. Corrugated-paper is widely used for packaging or shipping and becomes a kind of common solid waste. The novel attempts on the recycling of waste corrugated-paper packaging boxes may improve their economic and environmental interest.

Sorption is considered a removal method with easy operation and low cost widely used in wastewater treatment [6]. Although various types of sorbents have been developed and applied for water treatment during the past few decades, the development of novel and low-cost sorbents is still an important environmental research field. In recent years, carbon-based biochar, the carbonization of a variety of biomass and biomass-like materials under an oxygen-limited environment, has received much more attention because of its wide application such as carbon sequestration [7], soil improvement [8-9], and wastewater treatment [10-11]. Biochar has been validated as a renewable, low-cost and sustainable adsorbent for the removal of aqueous organic and inorganic contaminants [12-13]. However, the sorption performance of many pristine biochars derived from agricultural and forest biomass was relatively low [13]. Previous research confirms that the impregnation of minerals or metal oxides in biochar enhances significantly the sorption capacities of contaminants [14]. For example, Fe-impregnated biochar, prepared through a novel method that directly hydrolyzes iron salt onto hickory biochar was investigated for its performance as a low-cost arsenic (As) sorbent [15]. The mineral or metal ions' impregnation into the raw agricultural and forest biomass is a tedious step for the preparation of biochars due to its low adsorption capacities for mineral or metal ions. Waste paper is a subsistent mixture of organic matters (e.g., cellulose and/or inorganic adhesives) and mineral fillers (e.g., calcium carbonate and/or aluminosilicates) [1]. Therefore, the cost for the impregnation process can be ignored when the waste papers were carbonized. Our previous study shows that the carbonized waste-art-paper showed high sorption capacity of aqueous Pb(II) [16]. Therefore, the direct carbonization of waste paper may be a low-cost method for developing novel adsorbents.

In this study, waste-corrugated cardboard boxes were carbonized at temperatures of 300, 450, and 600°C, and the basic physicochemical properties of the resultant biochars were characterized. Batch experiments were conducted to examine sorption behavior of heavy metals (e.g., Pb(II), Cd(II), and Zn(II)), and organic dyes (e.g., methylene blue, or MB) onto the pristine biochars. The objectives of this work were: 1) to prepare and characterize the adsorbents – biochars – from the waste corrugated paper packaging boxes and 2) to explore the sorption performance of the resultant biochars for heavy metals and organic dyes, respectively. The simple treatment of waste-corrugated cardboard boxes to obtain highly efficient sorbent may offer a new method for the recycling and reuse of waste paper.

Experimental

Chemical Reagents

All the chemical reagents used were of analytic grade and solutions were prepared using ultrapure water (18.3 MΩ*cm) from Milli-Q Advantage A10 (Millipore, USA). Cadmium chloride ($\text{CdCl}_2 \cdot 2.5\text{H}_2\text{O}$), lead nitrate ($\text{Pb}(\text{NO}_3)_2$), zinc nitrate ($\text{Zn}(\text{NO}_3)_2 \cdot 6\text{H}_2\text{O}$), potassium nitrate (KNO_3), nitric acid (HNO_3), sodium hydroxide (NaOH), and methylene blue ($\text{C}_{16}\text{H}_{18}\text{ClN}_3\text{S}$) (MB) were purchased from Sinopharm Chemical Reagent Co., Ltd. All the lab ware was soaked in dilute nitric acid at least overnight, thoroughly flushed with tap water, and then with ultrapure water.

Preparation of Biochars

Waste corrugated-paper packaging boxes were collected from our lab and a local supermarket. They were then snipped to fragments (about 2×5 cm) using scissors. This feedstock was pyrolyzed under oxygen-limited condition in a muffle furnace (CIMO, SX₂-4-10, China) at peak temperature of 300, 450, and 600°C. The temperature was raised at a rate of 10°C min⁻¹ and held at the peak for 2 h. The obtained biochars were sieved with 18-mesh and 60-mesh nylon sieves to obtain 0.250-1.00 mm fraction, marked as CB300, CB450, and CB600, respectively, and stored for further investigation.

Characterization of Biochars

Contents of carbon (C), hydrogen (H), and nitrogen (N) in the pristine biochar samples were determined using a CHN Elemental Analyzer (Carlo-Erba NA-1500). Mineral elements were analyzed with an ICP-OES (PerkinElmer, Optima 5300DV, USA) after ashing at 360°C and acid dissolution. Specific surface areas of the biochar samples were measured with a surface area analyzer (BET, ASAP20, Micromeritics, Ltd., USA) using N₂ adsorption methods. Points of zero charge (pH_{pzc}) were measured by modified pH drift method as the previous literature [17]. Infrared spectrogram of the pristine biochars was measured by Fourier-transformed infrared spectroscopy (FTIR) (NEXUS870, NICOLET, USA) for characterizing the functional groups present in the pristine biochars. A powder X-ray diffractometer (XRD) was used to identify the crystal structure in the pristine and the heavy metal-adsorbed biochars.

Batch Sorption Experiments

Sorption isotherms of Cd(II), Pb(II), Zn(II), and MB onto the biochars were studied at room temperature (22±2°C) by adding 0.05 g biochar sample to a 50 mL plastic centrifuge tube containing 25 mL solution of Cd(II), Pb(II), Zn(II), or MB, respectively. According to our pre-experiments, initial concentrations of Cd(II)

ranged from 1 to 50 mg L⁻¹. Initial concentrations of Pb(II) ranged from 20 to 300 mg L⁻¹ for CB300, 50 to 1,000 mg L⁻¹ for CB450, and 200 to 1,500 mg L⁻¹ for CB600, respectively. Initial concentrations of Zn(II) ranged from 5 to 80 mg L⁻¹ for CB300, 20 to 300 mg L⁻¹ for CB450, and 50 to 500 mg L⁻¹ for CB600, respectively. MB initial concentration ranged from 5 to 150 mg·L⁻¹. Initial pH of Pb(II)/Cd(II)/Zn(II) solution was measured using a pH meter. The tubes were shaken in a rotating disk for 24 h to arrive at the sorption equilibrium. After centrifugation and filtration, final pH values of the filtrated solutions were determined by the pH meter. Concentrations of heavy metal ions (Cd²⁺, Pb²⁺ and Zn²⁺) in the filtrates were determined by using an ICP–OES (PerkinElmer, Optima 5300DV, USA). Equilibrium concentration of MB was measure using an ultraviolet spectrophotometer (PHILES, T-6, China) at 663 nm and pH 7.0 buffer systems. The amount of Cd(II), Pb(II), Zn(II), and MB sorbed was calculated using $q_e = [(C_0 - C_e) V]/m$, where C_0 and C_e are the initial and equilibrium concentrations of metal ions or MB (mg L⁻¹), respectively; V is the volume of the solution (L); and m is the mass of biochar (g).

An appropriate concentration of Cd(II), Pb(II), Zn(II), or MB for the kinetic sorption experiments were selected according to their sorption isotherms to avoid full adsorption at the beginning of the experiments or high residual concentrations. The kinetic sorption experiments were also carried out at room temperature (22±2°C) by adding 0.05 g biochar sample to 50 mL plastic centrifuge tube containing 25 mL of Cd(II), Pb(II), Zn(II), or MB. The initial concentrations of Cd(II), Pb(II), Zn(II), and MB were 30 mg L⁻¹, 1,000 mg·L⁻¹, 500 mg L⁻¹, and 50 mg L⁻¹, respectively. Initial solution pH was set at 5.0±0.2 for Cd(II), Pb(II), and Zn(II), and 6.5±0.2 for MB solution adjusted using 0.01 M NaOH or HNO₃ and measured using the pH meter. Centrifuge tubes were sealed and agitated in a rotary shaker. At the end time of 1 min, 5 min, 10 min, 20 min, 30 min, 1 h, 2 h, 4 h, 8 h, 16 h, and 24 h, the mixture was immediately centrifuged at 4,000 rpm and filtered through 0.45-µm pore size

nylon membranes. The amount of Cd(II), Pb(II), Zn(II), or MB sorbed was calculated using $q_t = [(C_0 - C_t) V]/m$, where C_t is the concentrations of heavy metals or MB (mg L⁻¹) at time of t .

Recovery of Adsorbed Heavy Metals

Acid-extraction experiments were carried out at room temperature (22±2°C) to recover heavy metal ions from the post-sorption (heavy metal-laden) biochars. In order to obtain heavy metal-laden biochars, 0.05 g biochar was mixed with 25 mL heavy metal solution of 20 mg L⁻¹ containing Cd(II) for CB300 and CB450, and 50 mg L⁻¹ for CB600; Pb(II) of 50 mg L⁻¹ for CB300, 500 mg L⁻¹ for CB450, and 1,200 mg L⁻¹ for CB600; Zn(II) of 50 mg L⁻¹ for CB300, and 500 mg L⁻¹ for CB450 and CB600. The mixed solution was shaken for 24 h in a rotary shaker. After centrifugation and filtration, the residue was washed using deionized (DI) water 3 times and dried at 70°C in a drying oven (CIMO, DHG-903385-III, China) for 12 h. Each post-sorption biochar sample was soaked in 3 mL 1.0 M HNO₃ solution for 1 h. The Cd(II), Pb(II), and Zn(II) concentrations in the leaching solution were measured by using ICP-OES. The desorption rate of heavy metal was calculated using $D(\%) = C_d \times V \times 100 / q_e$, where D is the desorption rate (%); C_d is the concentration of Cd(II), Pb(II), or Zn(II) in the leaching agent (mg L⁻¹); V is the volume of 1.0 M HNO₃ solution (L); and q_e is the equilibrium adsorption capacity (mg g⁻¹).

Results and Discussion

Characterization of Biochars

Basic Properties of the Pristine Biochars

The yields of waste corrugated-paper biochars at 300, 450, and 600°C were 48.1%, 30.1%, and 26.7%, respectively (Table 1), which were consistent with previous reports about decreasing yield with the

Table 1. Yield (%), ash and elemental contents (%), pore volume (cm³ g⁻¹), pore size(nm), and surface area (m² g⁻¹) of the pristine biochars.

	Yield	C	H	O ^a	N	H/C	(N+O)/C
CB300	48.1	49.6	4.60	29.1	0.25	1.113	0.444
CB450	30.1	55.9	2.66	8.16	0.080	0.571	0.111
CB600	26.7	60.0	1.75	0.94	0.31	0.350	0.0162
	Ash	Ca	Mg	Al	Surface area ^b	Pore volume ^c	Pore size ^d
CB300	16.5	1.78	0.169	0.955	3.47/1.32	0.0158/0.0147	18.2/44.6
CB450	33.2	4.90	0.522	1.99	27.5/15.1	0.0338/0.0285	4.91/7.52
CB600	37.0	4.11	0.413	2.40	270/65.4	0.158/0.0621	2.34/3.80

^aCalculated by mass difference between the total mass and the summation of CHN and ash of a sample, ^bBET/BJH, ^cTotal/BJH,

^dAve/BJH

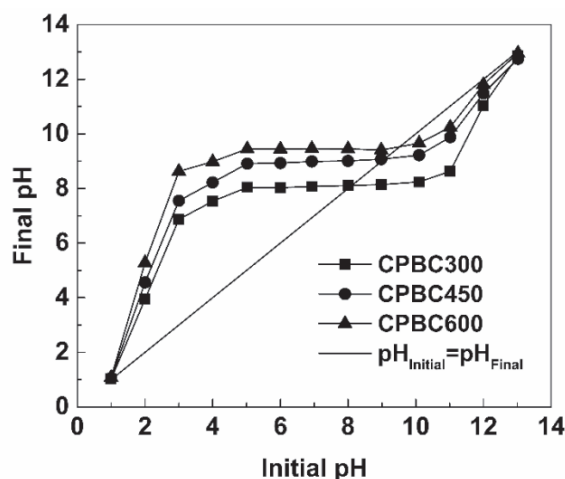


Fig. 1. pH_{pzc} of the resultant biochars.

increasing pyrolysis temperature [13]. CHN element contents and ash content of the pristine biochars were also shown in Table 1. In general, the C and ash content of the pristine biochar increased with the increasing pyrolysis temperature, while O and H contents inversely decreased. This indicated that the pristine biochar carbonized at high temperature had higher contents of graphite carbon and ash. For example, CB600 showed the highest contents of C (60.0%) and ash (37.0%). Atomic ratio of H/C decreased from 1.11 to 0.35, suggesting the strong carbonization and high aromaticity of the pristine biochars at high pyrolysis temperature [18-19]. The atomic ratio of (N+O)/C also decreased from 0.447 to 0.017, reflecting a decreased polar-group content with the increasing pyrolysis temperature. The dominant mineral elements in the pristine biochars were Ca, Al, and Mg. The Ca, Al, and Mg contents in CB450 and CB600 were obviously higher than that in CB300, which meant different mineral contents due to high pyrolysis temperature and low pyrolysis temperature.

pH_{pzc} is an important indicator of the net surface charge and preference for ionic species of a sorbent.

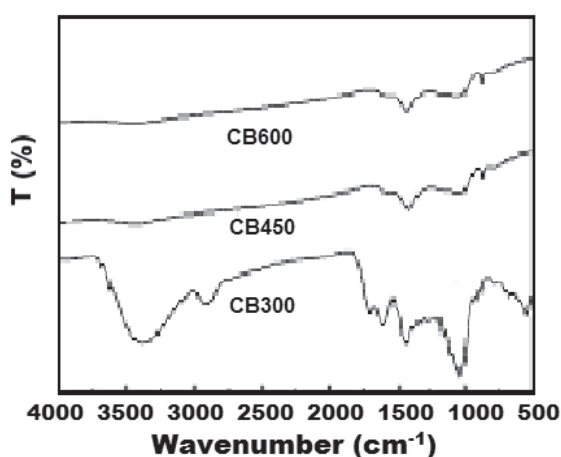


Fig. 2. FT-IR spectra of the resultant biochars.

The pH_{pzc} curves of the pristine biochars are shown in Fig. 1. Obviously, the pH_{pzc} values of three pristine biochars were quite similar, ranging from 8.0-9.5. The pH_{pzc} values of the pristine biochars increased with the increasing pyrolysis temperature. Solution pH lower than pH_{pzc} means positive surface charges of the resultant biochars, while the opposite result shows negative surface charges, which is easy to adsorb cations [20].

The BET and BJH surface areas were listed in Table 1. The BET and BJH surface area aggrandized with the increase of pyrolysis temperature. The total and BJH pore volume also have the same variation trend. However, the average and BJH pore size decrease with the increasing pyrolysis temperature. This was similar to a recent report [13].

FTIR Spectra of the Pristine Biochars

FT-IR spectra of the pristine biochars are shown in Fig. 2. The broadband peak at 3,000 to 3,700 cm^{-1} (O-H stretching vibrations of hydrogen bonded hydroxyl groups) and serial peaks at 1,600 to 1,800 cm^{-1} (C=O stretching vibrations) in the pristine biochars became weaker at high pyrolysis temperature, which was indicative of a decrease of oxygen-containing functional group (similar to the result of element content). The infrared absorption band around 1,425 cm^{-1} was assigned to the stretching vibration band of CO_3^{2-} [21], and the peak at 1,000 cm^{-1} in CB300 was attributed to the stretching vibration band of C-O. With the increasing pyrolysis temperature the peaks were reduced (Fig. 1), suggesting the breakdown of the functional groups due to high pyrolysis temperature.

XRD Spectra of the Pristine Biochars and Heavy Metal-Sorbed Biochars

The XRD spectra of the pristine biochars are shown in Fig. 3a. The patterns show that there was an obvious change of the components in the pristine biochars under different pyrolysis temperatures. The strong peak corresponding to calcium carbonate (CaCO_3 , PDF#05-0586) observed at 29.38° ($d = 3.04\text{\AA}$) in CB600 was stronger than those in CB300 and CB450, which indicated that high pyrolysis temperature could lead to the increasing content of CaCO_3 in the pristine biochars, and was consistent with the previous reports [22]. Otherwise, a relatively weak peak at 9.40° ($d = 9.401\text{\AA}$) in all 3 pristine biochars was attributed to talcum ($\text{Mg}_3\text{Si}_4\text{O}_{10}(\text{OH})_2$, PDF#13-0558). However, the weak peak at 12.34° ($d = 7.17\text{\AA}$) corresponding to kaolinite ($\text{Al}_2\text{Si}_2\text{O}_5(\text{OH})_4$) was only observed in CB300 and CB450. In addition, the quartz peak at 26.62° ($d = 3.35\text{\AA}$) was only observed in CB450. This result suggested that the main mineral in waste corrugated-paper biochars were calcium carbonate and a little clay mineral.

The XRD spectra of heavy metal-sorbed biochars (CB600-Pb, CB600-Zn, and CB600-Cd) are shown in Fig. 3b as a series of new strong peaks that could be

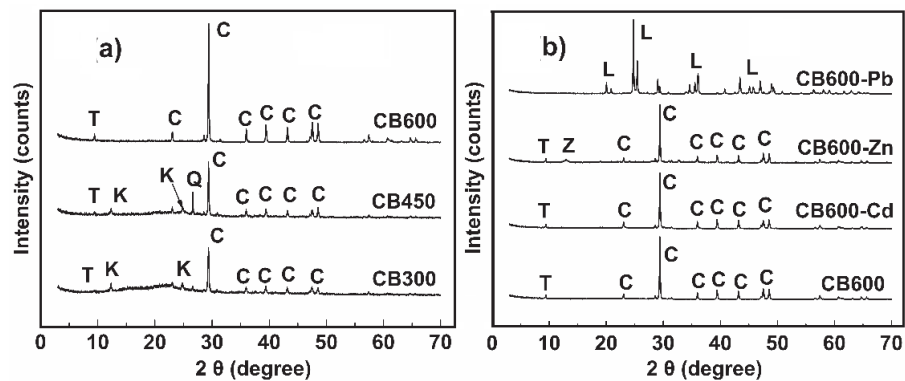


Fig. 3. XRD spectra of the pristine biochars a) and metal-laden biochars b) (C: calcium carbonate, K: kaolinite, T: talcum, Q: quartz, L: lead carbonate, Z: basic zinc carbonate)

distinctly observed in Pb-sorbed biochar (CB600-Pb). A strong peak at 24.78° ($d = 3.59 \text{ \AA}$) and a weak peak 29.04° ($d = 3.07 \text{ \AA}$) were identified as lead carbonate (PbCO_3), and a relatively weak peak at 36.1° ($d = 2.49 \text{ \AA}$) was attributed to basic lead carbonate [$\text{Pb}_2\text{CO}_3(\text{OH})_2$] [21]. In addition, the intensity of the calcite peak was reduced dramatically after the Pb(II) sorption. In Zn-sorbed biochar (CB600-Zn), a new and weak peak at 12.90° ($d = 6.86 \text{ \AA}$) were identified as basic zinc carbonate [$\text{Zn}_2(\text{OH})_2\text{CO}_3$]. However, no obvious new peak appeared in Cd-sorbed biochar, which may be due to the relatively low content of Cd sorbed that could not be detected by XRD. These results confirmed that the removal of Pb(II) and Zn(II) by the waste corrugated-paper biochar was mainly controlled by the precipitation mechanism through the reaction between calcite with Pb(II) and Zn(II).

Sorption Isotherms

The sorption isotherms are shown in Fig. 4. The sorption amount of the metal ions (Pb(II), Zn(II), and Cd(II)) onto the pristine biochars increased rapidly, and then arrived at a platform with the increasing equilibrium concentrations of Pb(II), Zn(II), or Cd(II) (Fig. 4). Fig. 4 shows that the equilibrium adsorption capacities for Pb(II) were in the order of $\text{CB600} > \text{CB450} > \text{CB300}$ and the maximum equilibrium adsorption capacities of CB600 were about 50 times higher than that of CB300. Therefore, the pyrolysis temperature had significant influence on the maximum equilibrium adsorption capacities of waste corrugated-paper biochars, which was consistent with the results of biochars derived from other biomass feedstock [23-24]. Zn(II) and Cd(II) showed the similar adsorption processing as Pb(II)

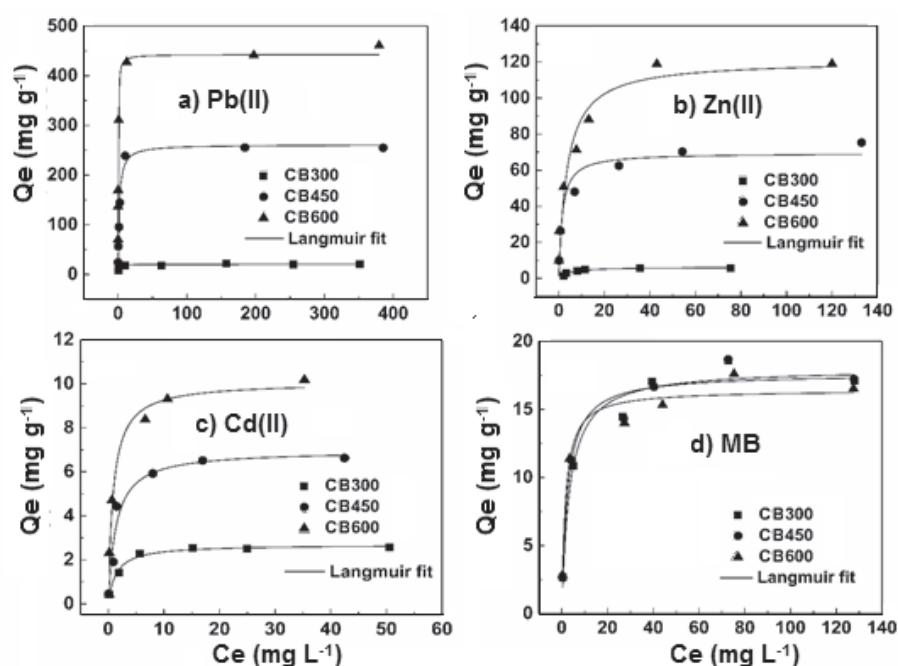


Fig. 4. Sorption isotherms of Pb(II) a), Zn(II) b), Cd(II) c), and methylene blue d) onto biochars.

Table 2. Isotherm model parameters for Pb(II), Zn(II), Cd(II), and MB sorption onto the tested biochars.

Adsorbates	Adsorbents	$C_e/q_e = C_e/q_m + 1/(K_L \times q_m)$ Langmuir model			$\lg q_m = \lg K_F + (1/n) \lg C_e$ Freundlich model		
		q_m	K_L	R^2	K_F	n	R^2
Pb(II)	CB300	15.9	0.042	0.978	7.21	8.79	0.876
	CB450	256	0.889	0.999	83.1	4.10	0.874
	CB600	458	1.06	0.999	208	5.86	0.772
Zn(II)	CB300	6.09	0.240	0.997	1.64	2.92	0.738
	CB450	76.2	0.333	0.998	24.2	3.70	0.949
	CB600	146	0.194	0.997	35.5	2.87	0.980
Cd(II)	CB300	2.61	1.02	0.999	0.958	3.11	0.872
	CB450	6.86	0.769	0.999	2.01	2.34	0.869
	CB600	10.7	0.572	0.993	2.94	2.20	0.717
MB	CB300	17.8	0.376	0.995	4.53	3.02	0.905
	CB450	17.9	0.375	0.995	4.87	3.19	0.894
	CB600	17.1	0.372	0.996	5.16	3.51	0.868

q_m : maximum adsorption capacity (mg g^{-1}), K_L : Langmuir constant (L mg^{-1}), K_F : affinity coefficient related to the bonding energy ($\text{mg}^{(1-1/n)} \text{L}^{1/n} \text{g}^{-1}$), n : the heterogeneity factor representing bond distribution

(Fig. 4), and the equilibrium adsorption capacities also increased with the increasing pyrolysis temperature (Fig. 4). Therefore, it can be concluded that the pyrolysis temperatures were the important parameters for the adsorption performance of the pristine biochars. Sorption isotherms of MB onto the pristine biochars are also shown in Fig. 4. The sorption of MB differed greatly from that of Pb(II), Zn(II), and Cd(II) (Fig. 4). Fig. 4 showed the similar adsorption capacities

of CB600, CB450, and CB300 for MB, so the adsorption mechanism of MB was different from that of the heavy metal ions.

For better understanding the sorption process, the Langmuir and Freundlich models were used to fit experimental data (Table 2). All Langmuir model coefficients (>0.97) were higher than Freundlich model coefficients, suggesting a better fitting with the Langmuir model. The Langmuir maximum sorption capacity of

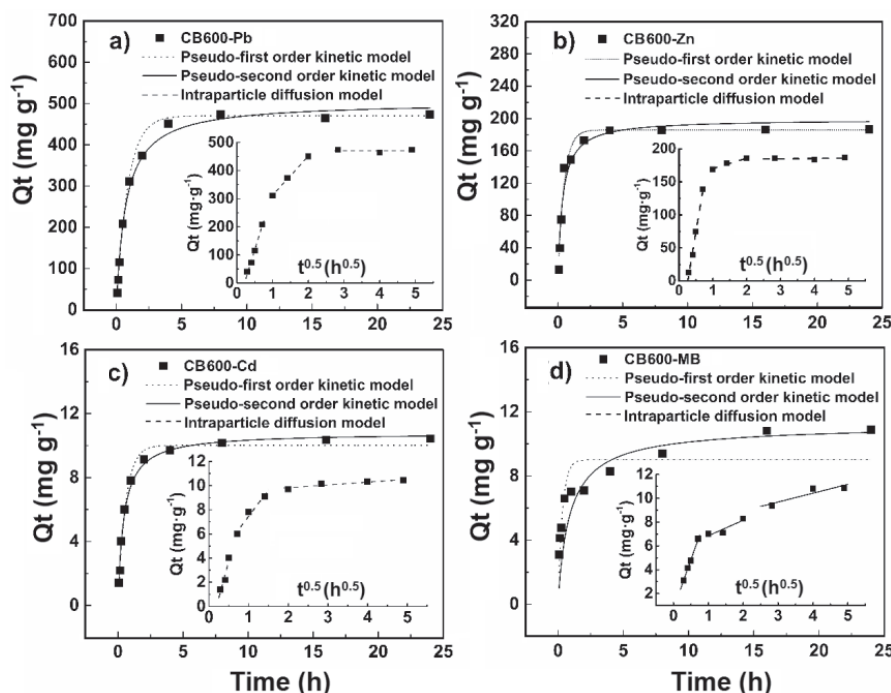


Fig. 5. Sorption kinetics of Pb(II) a), Zn(II) b), Cd(II) c), and methylene blue d) onto CB600.

Table 3. Kinetic model parameters for Pb(II), Zn(II), Cd(II), and MB sorption onto CB600.

	$q_{e,exp}$	Pseudo first-order $1/q_t = 1/q_e + k_1/(q_e t)$			Pseudo second-order $t/q_t = 1/[(q_e)^2 \times k_2] + t/q_e$			Intraparticle diffusion $q_t = K_p \times t^{0.5} + C$		
		$Q_{e,cal}$	k_1	R^2	$Q_{e,cal}$	k_2	R^2	K_p	C	R^2
Pb(II)	484	470	1.15	0.996	489	3.03	0.999	409	-85.8	0.989
Zn(II)	187	185	2.13	0.975	190	13.7	0.998	306	-79.4	0.994
Cd(II)	10.4	10.0	1.70	0.987	10.6	21.6	0.999	12.1	-12.3	0.910
MB	10.8	9.01	3.00	0.681	11.1	0.109	0.996	8.32	0.683	0.998

$q_{e,exp}$: experimental equilibrium adsorption capacity (mg g^{-1}), $q_{e,cal}$: calculated equilibrium adsorption capacity (mg g^{-1}), k_1 : pseudo first-order apparent adsorption rate constants (h^{-1}), k_2 : pseudo second-order apparent adsorption rate constants ($\text{mg mg}^{-1} \text{h}^{-1}$), K_p : intraparticle diffusion rate constants ($\text{mg g h}^{-0.5}$), C : constant (mg g^{-1}).

CB600 was 458 mg g^{-1} for Pb(II), 146 mg g^{-1} for Zn(II), and 10.7 mg g^{-1} for Cd(II), respectively (Fig. 4), indicating the elemental dependent. The sorption capacities of these heavy metal ions for CB600 were much higher than those for other carbon-based sorbents, including activated carbon reported in the literature [25-28]. So the waste corrugated-paper biochars can be used as an effective sorbent for the removal of heavy metal ions from aqueous solutions.

Sorption Kinetics

Adsorption kinetics of metals from CB600, which had maximum adsorption capacity for Pb(II), Zn(II), Cd(II), and MB among the 3 biochars, are shown in Fig. 5. Sorption amount of the 4 sorbates increased rapidly with contact time in the first 2 hours and then the increase of the adsorption amount slowed down. The sorption of the sorbates reached equilibrium in 5 h except for MB, which needed about 10 h. Pseudo first-order and pseudo second-order models, and the intraparticle diffusion model were used to fit the adsorption data and the parameters are listed in Table 3. The calculated equilibrium sorption capacities ($q_{e,cal}$) by pseudo second-

order of Pb(II), Zn(II), Cd(II), and MB were 489, 190, 10.6, and 11.1 mg g^{-1} , respectively, which were closer to the experimental q_e values ($q_{e,exp}$). The correlation coefficient values (R^2) of the pseudo second-order model were higher than that of the pseudo first-order model. These suggested that the pseudo second-order model provided a better fit for Pb(II), Zn(II), Cd(II), and MB adsorption than the pseudo first-order model (Fig. 5). Moreover, liner fitting results by intraparticle diffusion model were also shown in Fig. 5 and Table 3. It is reported that the initial straight line passing through the origin represented the external mass transfer region or surface adsorption [29]. Fig. 5 showed that the linear plot did not pass through the origin, which indicated that the intraparticle diffusion was not the only rate controlling step, and that boundary layer diffusion was involved. Therefore, Pb(II), Zn(II), Cd(II), and MB adsorption onto CB600 might occur by a multi-step adsorption process. This is similar to previous reports [29].

Desorption of Pb(II), Zn(II), and Cd(II)

Desorption rates of Pb(II), Zn(II), and Cd(II) from the metal-laden biochars are presented in Fig. 6. We found that more than 90% of absorbed Pb(II), Zn(II), and Cd(II) could be desorbed from the biochars using 1 M HNO_3 , which suggested that Pb(II), Zn(II), and Cd(II) could be recycled well by immersing the metal-laden biochars in 1M HNO_3 solution.

Conclusions

Biochars were derived from waste corrugated-paper through slow pyrolysis under 300, 450, and 600°C. The basic physicochemical properties and sorption performance of the resultant biochars were influenced greatly by the pyrolysis temperature. Biochar obtained at high pyrolysis temperature (CB600) exhibited high specific surface area and high mineral contents. Moreover, high-temperature biochar (600°C) showed high removal of lead, zinc, and cadmium from aqueous solutions than low-temperature biochars did (300

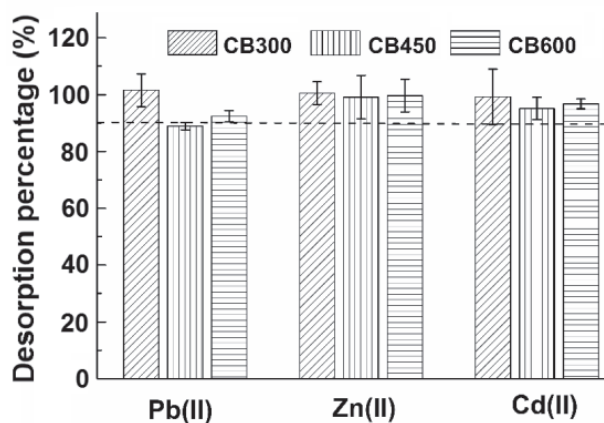


Fig. 6. Desorption of Pb(II), Zn(II), and Cd(II) from the metal-laden biochars by 1 M HNO_3 .

and 450°C). The sorption of Pb(II) or Zn(II) onto the high-temperature biochars (CB600) was mainly controlled by a chemical precipitation mechanism while the sorption of MB contributed to electrostatic adsorption. Finally, dilute acid extraction successfully recovered the sorbed heavy metal from the exhausted sorbent. In a word, simple preparation and high removal efficiency of heavy metal ions make the waste corrugated-paper biochars promising cost-effective sorbents for wastewater treatment and it is helpful in developing novel recovery methods for waste corrugated cardboard boxes.

Acknowledgements

Our work was partly supported by the National Natural Science Fund of China (No. 21677075) and the Culture Project of International Cooperation and Exchange of Nanjing Tech University.

References

- PIVNENKO K., ERIKSSON E., ASTRUP T.F. Waste paper for recycling: Overview and identification of potentially critical substances. *Waste Manage* **45**, 134, **2015**.
- ADHIKARI C.R., PARAJULI D., INOUE K., OHTO K., KAWAKITA H., HARADA H. Recovery of precious metals by using chemically modified waste paper. *New J Chem* **32**, 1634, **2008**.
- KALPANA D., CHO S.H., LEE S.B., LEE Y.S., MISRA R., RENGANATHAN N.G. Recycled waste paper - A new source of raw material for electric double-layer capacitors. *J Power Sources* **190**, 587, **2009**.
- MA Y., HUMMEL M., MAATTANEN M., SARKILAHTI A., HARLIN A., SIXTA H. Upcycling of waste paper and cardboard to textiles. *Green Chem* **18**, 858, **2016**.
- GHORBEL L., ROUISSI T., BRAR S.K., LOPEZ-GONZALEZ D., RAMIREZ A.A., GODBOUT S. Value-added performance of processed cardboard and farm breeding compost by pyrolysis. *Waste Manage* **38**, 164, **2015**.
- AZIMI A., AZARIA., REZAKAZEMI M., ANSARPOUR M. Removal of heavy metals from industrial wastewaters: A review. *Chembioeng Rev* **4**, 37, **2017**.
- MATOVIC D. Biochar as a viable carbon sequestration option: Global and Canadian perspective. *Energy* **36**, 2011, **2011**.
- SOHI S.P., KRULL E., LOPEZ-CAPEL E., BOL R. A review of biochar and its use and function in soil. In Sparks D.L. (ed.): *Advances in agronomy*, Vol. 105, Burlington: Academic Press, 2010, 47, **2010**.
- MAYER Z.A., ELTOM Y., STENNETT D., SCHRODER E., APFELBACHER A., HORNUNG A. Characterization of engineered biochar for soil management. *Environ Prog Sustain* **33**, 490, **2014**.
- DING Z., HU X., WAN Y., WANG S., GAO B. Removal of lead, copper, cadmium, zinc, and nickel from aqueous solutions by alkali-modified biochar: Batch and column tests. *J Ind Eng Chem* **33**, 239, **2016**.
- INYANG M.I., GAO B., YAO Y., XUE Y.W., ZIMMERMAN A., MOSA A., PULLAMMANAPPALLIL P., OK Y.S., CAO X.D. A review of biochar as a low-cost adsorbent for aqueous heavy metal removal. *Crit Rev Env Sci Tec* **46**, 406, **2016**.
- AHMED M.B., ZHOU J.L., NGO H.H., GUO W., CHEN M. Progress in the preparation and application of modified biochar for improved contaminant removal from water and wastewater. *Bioresource Technol* **214**, 836, **2016**.
- MOHAN D., SARSWAT A., OK Y.S., PITTMAN C.U. Organic and inorganic contaminants removal from water with biochar, a renewable, low cost and sustainable adsorbent - A critical review. *Bioresource Technol* **160**, 191, **2014**.
- MICHALEKOVA-RICHVEISOVA B., FRISTAK V., PIPISKA M., DURISKA L., MORENO-JIMENEZ E., SOJA G. Iron-impregnated biochars as effective phosphate sorption materials. *Environ Sci Pollut R* **24**, 463, **2017**.
- HU X., DING Z.H., ZIMMERMAN A.R., WANG S.S., GAO B. Batch and column sorption of arsenic onto iron-impregnated biochar synthesized through hydrolysis. *Water Res* **68**, 206, **2015**.
- XU X., HU X., DING Z., CHEN Y., GAO B. Waste-art-paper biochar as an effective sorbent for recovery of aqueous Pb(II) into value-added PbO nanoparticles. *Chem Eng J* **308**, 863, **2017**.
- FARIA P.C.C., ÖRF O J.J.M., PEREIRA M.F.R. Adsorption of anionic and cationic dyes on activated carbons with different surface chemistries. *Water Res* **38**, 2043, **2004**.
- BOGUSZ A., OLESZCZUK P., DOBROWOLSKI R. Application of laboratory prepared and commercially available biochars to adsorption of cadmium, copper and zinc ions from water. *Bioresource Technol* **196**, 540, **2015**.
- KEILUWEIT M., NICO P.S., JOHNSON M.G., KLEBER M. Dynamic molecular structure of plant biomass-derived black carbon (biochar). *Environ Sci Technol* **44**, 1247, **2010**.
- TAN X., LIU Y., ZENG G., XIN W., HU X., GU Y., YANG Z. Application of biochar for the removal of pollutants from aqueous solutions. *Chemosphere* **125**, 70, **2015**.
- XU X., CAO X., ZHAO L. Comparison of rice husk- and dairy manure-derived biochars for simultaneously removing heavy metals from aqueous solutions: Role of mineral components in biochars. *Chemosphere* **92**, 955, **2013**.
- YAO Y., GAO B., INYANG M., ZIMMERMAN A.R., CAO X., PULLAMMANAPPALLIL P., YANG L. Biochar derived from anaerobically digested sugar beet tailings: Characterization and phosphate removal potential. *Bioresource Technol* **102**, 6273, **2011**.
- TAN C., ZHANG Y., WANG H., LU W., ZHOU Z., ZHANG Y., REN L. Influence of pyrolysis temperature on characteristics and heavy metal adsorptive performance of biochar derived from municipal sewage sludge. *Bioresource Technol* **164C**, 47, **2014**.
- YANG G., WANG Z., XIAN Q., SHEN F., SUN C., ZHANG Y., WU J. Effects of pyrolysis temperature on the physicochemical properties of biochar derived from vermicompost and its potential use as an environmental amendment. *RSC Adv* **5**, 40117, **2015**.
- PYRZYNSKA K. Sorption of Cd(II) onto carbon-based materials-a comparative study. *Microchim Acta* **169**, 7, **2010**.
- DING W., DONG X., IME I.M., GAO B., MA L.Q. Pyrolytic temperatures impact lead sorption mechanisms by bagasse biochars. *Chemosphere* **105**, 68, **2014**.

27. JIANG S., HUANG L., NGUYEN T.A.H., OK Y.S., RUDOLPH V., YANG H., ZHANG D. Copper and zinc adsorption by softwood and hardwood biochars under elevated sulphate-induced salinity and acidic pH conditions. *Chemosphere* **142**, 64, **2016**.
28. DING Z., HU X., WU H. Multiple characterization for mechanistic insights of Pb(II) sorption onto biochars derived from herbaceous plant, biosolid, and livestock waste. *Bioresources* **12**, 6763, **2017**.
29. LIU N., CHARRUA A.B., WENG C.H., YUAN X., DING F. Characterization of biochars derived from agriculture wastes and their adsorptive removal of atrazine from aqueous solution: A comparative study. *Bioresource Technol* **198**, 55, **2015**.

